frontiers | Frontiers in Materials

ORIGINAL RESEARCH
published: 22 July 2022
doi: 10.3389/fmats.2022.959480

Three-Dimensional Simulation Platform for Optimal Designs of the MEMS Microphone

Jianbing Cai[1], Jian Zhou[1], Zhangbin Ji[1], Kaitao Tan[1], Yi Liu[2] and Yongqing Fu[3]*

[1]College of Mechanical and Vehicle Engineering, Hunan University, Changsha, China, [2]National Rail Transit Advanced Equipment Innovation Center, Zhuzhou, China, [3]Faculty of Engineering and Environment, Northumbria University, Newcastle Upon Tyne, United Kingdom

MEMS microphone has a wide range of application prospects in electronic devices such as mobile phones, headphones, and hearing aids due to its small size, low cost, and reliable performance. Research and development of MEMS microphones involves multiple thermo-electro-mechanical couplings among various physical and electrical fields. Unfortunately, there is not an accurate three-dimensional (3D) MEMS microphone simulation platform, which can be applied for the design of chip parameters and packaging characteristics. Herein, based on commercial COMSOL software, we have established a 3D simulation platform for MEMS microphones, which is used to systematically study the influences of geometric structure and physics parameters on the sensitivity and frequency responses of the microphone and consider the influences of packaging characteristics on the performance of the microphone. The simulation results are consistent with those obtained using a lumped element method, which proves the accuracy of the simulation platform. The platform can be used to design and explore new principles or mechanisms of MEMS microphone devices.

Keywords: MEMS, microphone, 3D simulation, frequency responses, sensitivity

OPEN ACCESS

Edited by:
Xufeng Dong,
Dalian University of Technology, China

Reviewed by:
Xuan Weipeng,
Hangzhou Dianzi University, China
Yunya Liu,
Xiangtan University, China

****Correspondence:***
Jian Zhou
jianzhou@hnu.edu.cn

Specialty section:
This article was submitted to Smart Materials, a section of the journal Frontiers in Materials

Received: *01 June 2022*
Accepted: *17 June 2022*
Published: *22 July 2022*

Citation:
Cai J, Zhou J, Ji Z, Tan K, Liu Y and Fu Y (2022) Three-Dimensional Simulation Platform for Optimal Designs of the MEMS Microphone. Front. Mater. 9:959480. doi: 10.3389/fmats.2022.959480

INTRODUCTION

Micro-electro-mechanical systems (MEMS) are micro-scale sensors and actuators manufactured by modern micro-manufacturing technology (Wang et al., 2009) within multi-disciplinary and multi-physics fields such as machinery, electronics, biology, acoustics, and energy (Bi-Qiang et al., 2006). Compared with conventional sensors, MEMS sensors have great advantages in terms of volume, price, properties, and capacity (Fitzgerald et al., 2021) and are gradually replacing those traditional sensors in many fields such as automotive, biomedical devices, and personal electronics. (Bogue and Review, 2013; Mohd Ghazali et al., 2020).

The microphone is one of the key acoustic-electric transducers which convert acoustic signals into electrical signals (Choe and Bulat, 2005; Arora et al., 2018). Proposed in 1962, electret capacitive microphones (ECMs) are low-cost, high-sensitivity, with a broadband, which have revolutionized the microphone industry (Kapps and Dobbins, 2014; Adorno et al., 2022). The ECMs have created built-in charges due to the existence of an electret layer (i.e., a thin plastic foil that can hold the charge) and are standard solutions for telephones and personal electronic products. The first MEMS microphone was introduced in 1983 (Ozdogan et al.,

2020). However, it was not until 2003 when the first silicon-based MEMS microphone became the mass production and Knowles launched the first SiSonic^{TM} MEMS microphone (Resound, 2014), which pioneered the development of the MEMS market. Compared with the ECMs, MEMS microphones are compatible with integrated circuits (IC) technology and surface mount technology (SMT) (Oh et al., 2021) and have shown much better mechanical shock resistance and anti-interference performance, which have gradually developed into the mainstream of microphones in the commercial market. Today, new types of MEMS microphones are still being developed in the market, and it is reported that the annual output of MEMS microphones is as high as billions (Zhang et al., 2021).

In order to meet the stringent requirements of different industries, a variety of MEMS microphone products have been developed, and the prototype of MEMS microphone for each demand has to be significantly shortened to reduce the development cycle and reduce the development cost. Therefore, an efficient design methodology and techniques are required. Common design methods for MEMS devices include the lumped element method (LEM) and the finite element method (FEM).

In 2017, Rufer et al. proposed an accurate lumped parameter equivalent circuit to simulate various configurations of capacitive microphones (Esteves et al., 2017). Studies have shown that this equivalent model can easily be adapted into other specific microscopic configurations. In 2019, Lee et al. (2019) proposed a dynamic open circuit sensitivity model based on electrical equivalent circuits, which has shown high accuracy and has produced results that are only ~2% different from the simulation results of FEM. Auliya et al. (2019) proposed a 2D finite element model to analyze the performance of MEMS microphones. The 2D model is used to simplify the calculation by applying axisymmetric conditions, which greatly reduces the application range of the model. In 2021, Shubham et al. (2021) demonstrated a MEMS microphone chip with flexible springs in the diaphragm and developed a lumped element model to predict the mechanical and electrical behavior of the microphone. Experiments show that there is a good correlation between the measured curve and the simulated curve.

The aforementioned equivalent methods have achieved good results in the prediction of the sensitivity and frequency response of the microphones, but there still exist quite different issues, because some parameters in these models require to be obtained by FEM or experiments, which is often inconvenient in the prototype design stage of MEMS microphones. Research and development of MEMS microphones involves multiple thermo-electro-mechanical couplings and various physical and electrical fields. Unfortunately, there is currently no any accurate and efficient three-dimensional (3D) MEMS microphone simulation platform, which can be applied for design of its chip parameters and packaging characteristics.

In this study, we proposed a 3D simulation platform for MEMS microphones using the commercial software COMSOL, and designed a set of parameters to describe the structure of the MEMS microphone. The sensitivity and frequency responses of the microphone were investigated using the proposed platform, and the accuracy of the platform was evaluated by comparing the obtained results with the simulation results using the LEM.

WORKING PRINCIPLE OF THE MICROPHONE

A typical MEMS microphone is composed of a MEMS chip, an ASIC chip, a printed circuit board, and a metal shell with an acoustic port, as illustrated in **Figure 1A,B**. The MEMS chip mainly includes a rigid backplane and an elastic thin diaphragm (Naderyan et al., 2021), which are normally made of polysilicon materials. There are a large number of air holes in the silicon backplane, which allow air to pass through in order to reduce air damping (Naderyan et al., 2020). The diaphragm also needs vent holes to balance the pressure between the front cavity and the back cavity. In a first approximation, as shown in the basic schematic illustration as shown in **Figure 1C**, the capacitive MEMS microphone sensor can be modeled as a parallel plate capacitor (Sant et al., 2019). In this model, the DC bias voltage V_{bias} is applied to the variable capacitor through a resistance R_{bias} with a maximum resistance value. The initial air gap height of the capacitor is d_0, the effective area is S, the accumulated charge of the capacitor is Q, and the initial capacitance is C_0. The large time constant makes the capacitor work in a constant charge mode.

When the acoustic pressure P (1Pa) is applied to the diaphragm to cause its vibration, the capacitance of this capacitor changes with a value of ΔC, when the air gap of the parallel plate is changed with Δd.

$$\Delta C = \frac{\varepsilon S}{d_0 - \Delta d} = \frac{\varepsilon S}{d_0}.\frac{1}{1 - \Delta d/d_0} = C_0.\frac{d_0}{d_0 - \Delta d}. \tag{1}$$

Since the charge of the parallel plate capacitor is assumed to be a constant, the output voltage ΔV of the capacitor will change with the capacitance value. An ASIC chip can be used to read the voltage on the capacitor plate and process it when needed.

$$\Delta V = \frac{Q}{\Delta C} = V_{bias}\frac{\Delta d}{d_0}. \tag{2}$$

The sensitivity of the sensor is the ratio of the specified output to the specified input. Therefore, the sensitivity of the microphone can be defined as

$$S_0 = \frac{\Delta V}{P} = \left(\frac{V_{bias}}{d_0}\right)\Delta d. \tag{3}$$

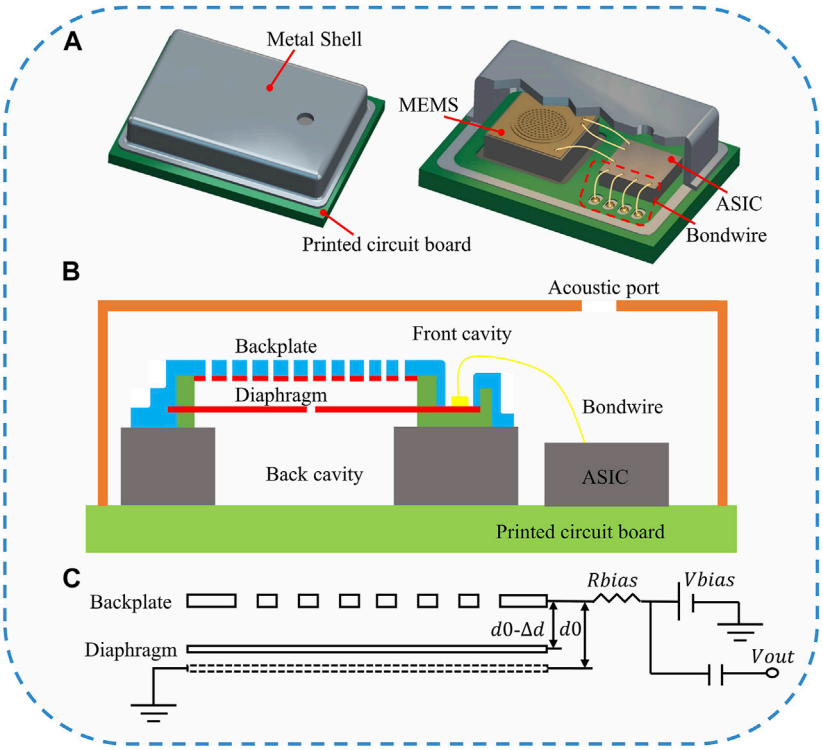

FIGURE 1 | (A) Scheme of a top port MEMS microphone. **(B)** Schematic cross-section of the MEMS microphone. **(C)** Principle of the MEMS microphone.

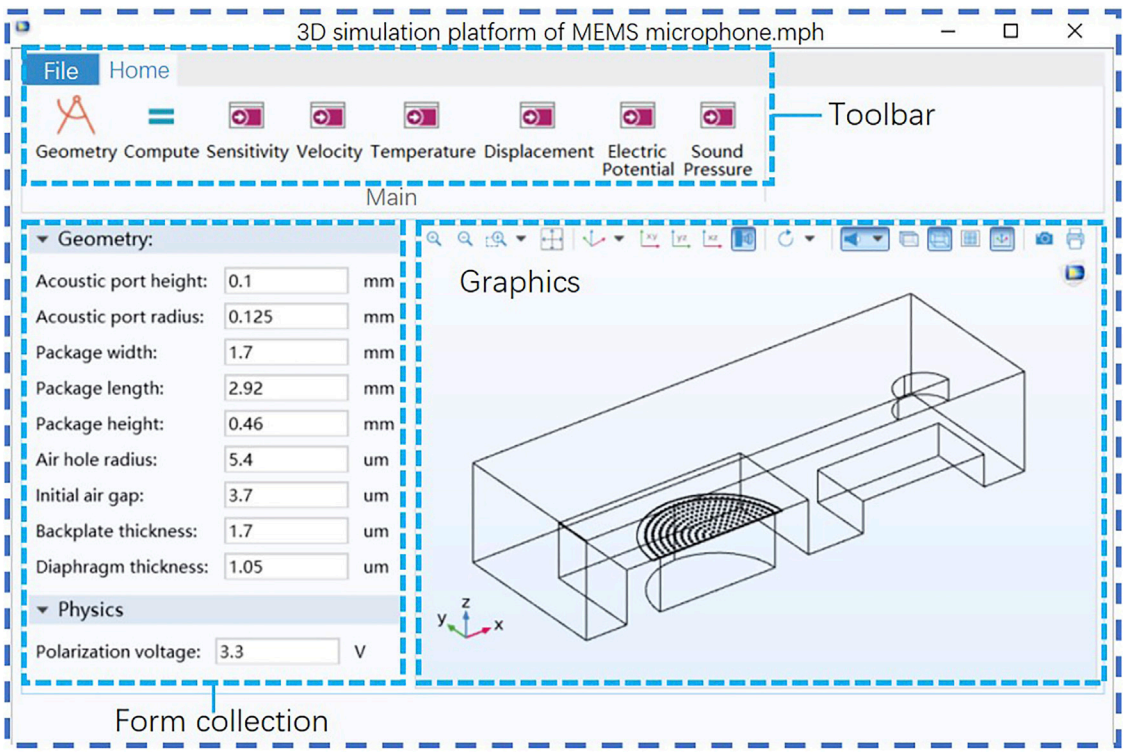

FIGURE 2 | Three-dimensional finite element simulation platform for MEMS microphones.

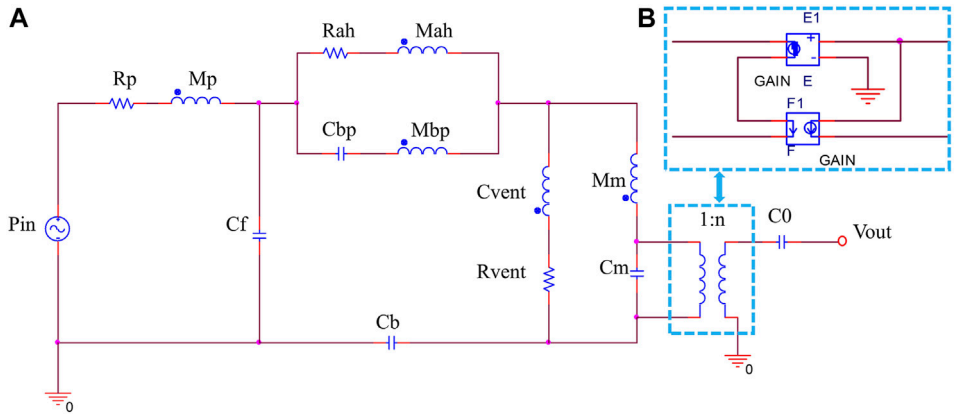

FIGURE 3 | (A) Lumped element equivalent circuit diagram of the MEMS microphone. **(B)** Ideal transformer model.

TABLE 1 | Description of the microphone acoustic lumped element in **Figure 3**.

Category	Symbol	Description	Units
Package acoustical parameters	R_p	Acoustic port resistance	$N \cdot s/m^5$
	M_p	Acoustic port inductance	$N \cdot s^2/m^5$
	C_f	Front cavity compliance	m^5/N
	C_b	Back cavity compliance	m^5/N
MEMS motor parameters	R_{ah}	Backplane hole resistance	$N \cdot s/m^5$
	R_{ag}	Air gap resistance	$N \cdot s/m^5$
	M_{ah}	Backplate hole inductance	$N \cdot s^2/m^5$
	C_{bp}	Backplate compliance	M^5/N
	M_{bp}	Backplate mass	kg/m^4
	R_{vent}	Vent resistance	$N \cdot s/m^5$
	M_{vent}	Vent inductance	$N \cdot s^2/m^5$
	C_m	Diaphragm compliance	m^5/N
	M_m	Diaphragm mass	kg/m^4
	n	Turns ratio	V/Pa

TABLE 2 | Pertinent dimensions and parameters used for the simulation of the MEMS microphone.

Referenced parameter value of the designed MEMS microphone			
Initial air gap	$3.7\mu m$	Front cavity volume	$1.23mm^3$
Air hole radius	$5.4\mu m$	Back cavity volume	$0.06mm^3$
Backplate radius	$320\mu m$	Acoustic port radius	$125\mu m$
Diaphragm radius	$285\mu m$	Acoustic port height	$100\mu m$
Air hole quantity	441	Diaphragm density	$2330kg/m^3$
Perforation ratio	0.125	Young's modulus of diaphragm	$160GPa$
Backplate thickness	$1.7\mu m$	Poisson's ratio of diaphragm	0.2
Diaphragm thickness	$1.05\mu m$	Bias voltage	$3.3V$
Initial capacitance	$0.58pF$	–	–

PROPOSED MODEL AND SIMULATION PLATFORM

In this work, a 3D FEM platform for MEMS microphones was proposed using the commercial COMSOL software, as shown in **Figure 2**. In this simulation platform, graphics can be used to show the geometry of the microphone model, a top toolbar provides geometry, calculation buttons, and presets for some drawing commands, and a form collection presents the modifiable model parameters. In order to reduce the calculation time, symmetrical boundary conditions are applied on the longitudinal section and only half of the MEMS microphone structure is modeled based on the symmetrical MEMS microphone structure. The study of MEMS microphone's sensitivity and frequency responses involve multi-physics fields such as "Thermoviscous Acoustics," "Membrane," "Electrostatics," and "Circuit."

In addition, a lumped element model was also developed to describe the dynamic behavior of the MEMS microphone and evaluate the sensitivity and frequency responses of the microphone, as shown in **Figure 3**. **Table 1** presents the description of each lumped element used in this model. The equivalent circuit model of our MEMS microphone was simulated in the simulation program with integrated circuit emphasis (SPICE), in which the transformer adopted the ideal

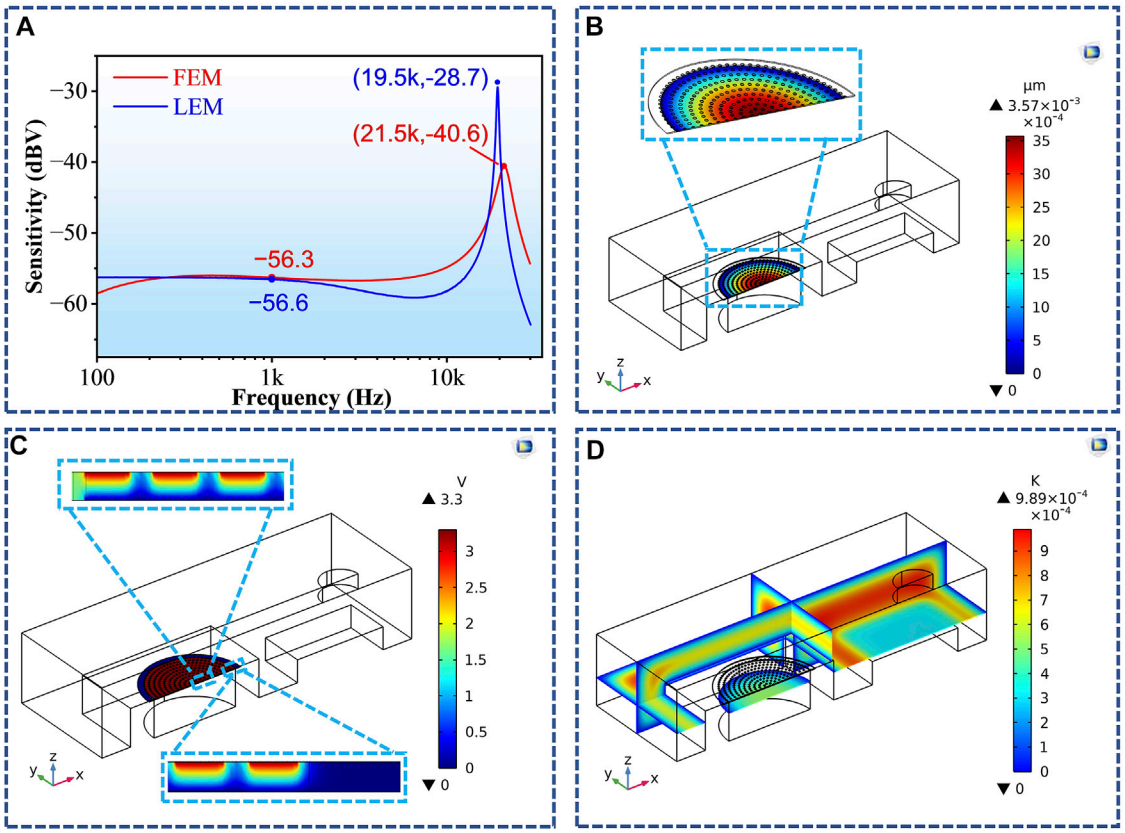

FIGURE 4 | (A) Comparison of the MEMS microphone frequency response obtained by the FEM and the LEM. **(B)** Displacement of the membrane at 1 kHz. **(C)** Electric potential. **(D)** Temperature oscillation amplitude distribution at 1 kHz.

transformer model composed of controlled sources. The geometric and material parameters of each part of the MEMS microphone are listed in **Table 2**.

Figure 4A shows the calculated results obtained by the FEM using COMSOL software and the LEM model, respectively, which show good consistency, demonstrating the efficiency, accuracy, and reliability of the 3D FEM platform. The sensitivity of the MEMS microphone at 1 kHz is ?56.3 dBV and ?56.6 dBV for the FEM model and LEM model, respectively, and the difference is only 0.5%. For both the FEM model and the LEM model, the change in sensitivity of frequency response is less than ± 3 dBV from 100 Hz to 12 kHz. The resonance frequencies are 21.5 and 19.5 kHz for the FEM model and the LEM model, respectively, indicating the consistency of the frequency results. The LEM model appears to show a relatively higher sensitivity at the resonance frequency. This is because in the lumped element model, the nonlinear dependence of capacitance on the diaphragm displacement is often overestimated by the piston approximation, leading to a significant overestimation of the spatial derivative of capacitance (Anzinger et al., 2021) and a higher sensitivity.

Visualization of calculation results makes designers more intuitive to find the deficiencies in the model, which is also one of the advantages of our new platform. **Figure 4b~d** and **Figure 5** show the results from the FEM simulation. **Figure 4B** shows the displacement distributions of the diaphragm under the simulation sound pressure of 1 Pa. The displacement at the center of the diaphragm is the largest, and the displacement on both sides decreases gradually. The displacement of the membrane at different times of 1 kHz is shown in **Figure 5**. **Figure 4C** depicts the potential of the symmetrical plane of the microphone motor, and the obtained results clearly show that the holes on the backplane will affect the field. It can be seen that the electric field has a very strong gradient in the area where the electrode is located, and it will be decreased outside that area. **Figure 4D**illustrates the temperature oscillation distribution at 1 kHz in the enclosure. Due to the isothermal boundary condition, the amplitude of the temperature oscillation becomes zero at the boundary between the enclosure and the surface of the silicon chip and reaches a peak at the region between the enclosure wall and the silicon chip, which is about 98.9 μK.

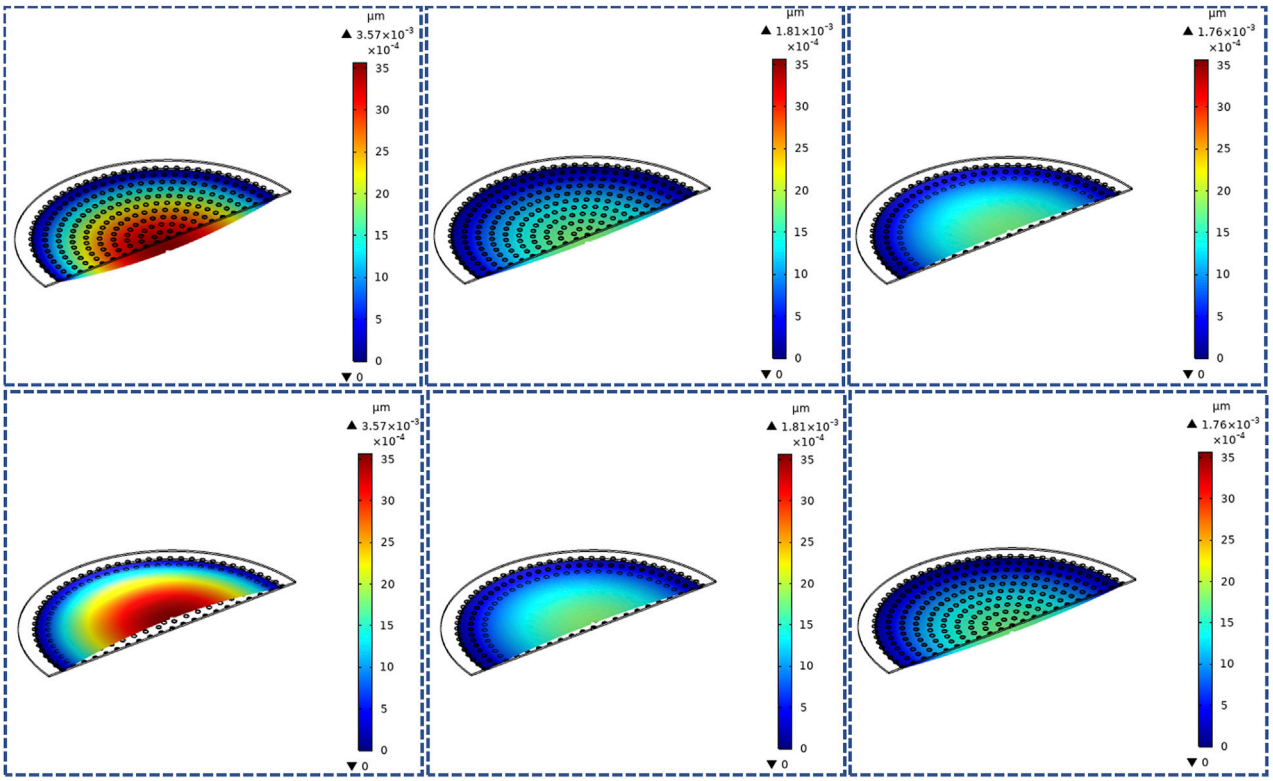

FIGURE 5 | Displacement of the membrane at different times of 1 kHz.

EFFECTS OF STRUCTURAL AND ELECTRICAL PARAMETERS AND PACKAGING CHARACTERISTICS ON FREQUENCY RESPONSES OF MEMS MICROPHONES

In order to ensure the universal capability of the established finite element platform for MEMS microphones, some parameters of the MEMS microphone were varied in the simulations. **Figure 6** describes the influences of air gap height (d_0), bias voltage (V_{bias}) and front cavity volume (V_f) on MEMS microphone frequency responses, respectively. The results obtained from the two methods have shown good consistency.

Figure 6A shows that the dynamic open circuit sensitivity is -58.5 dBV, -56.3 dBV, and -53.4 dBV at the gap heights of 4.7, 3.7, and 2.7 μm, respectively. **Figure 6C** shows the dynamic open circuit sensitivities of −56.3 dBV, −52.7 dBV, and −48.9 dBV at 3.3, 5.0, and 8.0 V bias, respectively. Results show that reducing air gap height or increasing bias voltage can improve the sensitivity of MEMS microphones, which is compatible with the prediction from **Eq. 3**. **Figure 6E** shows that when the volumes of the front cavity are 1.04 mm^3, 1.24 mm^3 and 1.47 mm^3, the sensitivity of the microphone is about—56.3 dBV, and the resonant frequencies are 23.0, 21.5, and 20.0 kHz, respectively. It can be seen that the smaller volume of the front cavity will result in smaller frequency responses and higher resonant frequencies of the microphone, mainly because of the acoustic port and the front cavity forming a Helmholtz resonator (Mackey et al., 2019).

Based on the aforementioned analysis, we can obtain the MEMS microphone with a dynamic open circuit sensitivity of −48.9 dBV at an air gap height of 3.7 μm, a bias voltage of 8.0 V, which is much higher than that (−55.4 dBV) in previous work (Lee et al., 2012).

CONCLUSION

In this study, we introduce a 3D simulation platform for MEMS microphone based on commercial COMSOL software, which can be used to study the influences of microphone geometric or physical parameters on its sensitivity and frequency responses. The results are in good agreement with those calculated by the LEM. The model is built with parameters of the inputs of the sensor, which can be readily changed by the designer. After the parameters have been changed, the model will be automatically reconstructed and meshed. The visualization of research results helps designers more intuitively find the shortcomings of the model, optimize and improve the model, and greatly promote the prototype design stage.

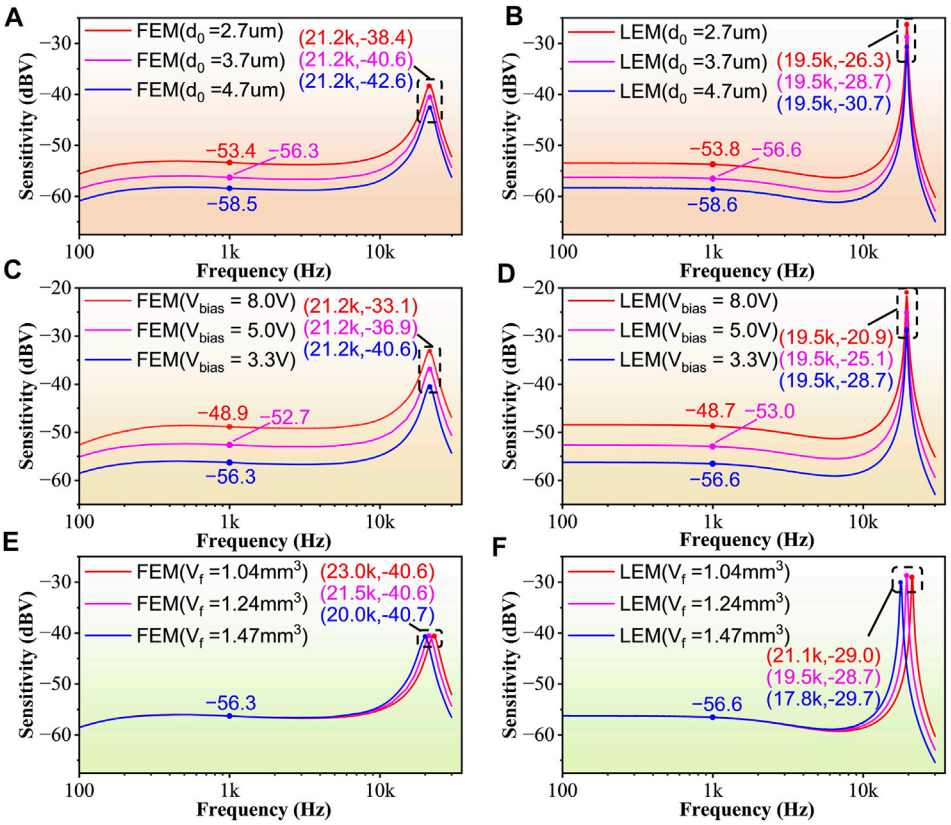

FIGURE 6 | Simulation of the frequency response of MEMS microphone with different parameters using the FEM and the LEM. **(A)** and **(B)** describe the influences of air gap heights d_0 change. **(C)** and **(D)** describe the influences of bias voltage V_{bias} variation. **(E)** and **(F)** describe the influences of the volume V_f change of the front cavity.

DATA AVAILABILITY STATEMENT

The data in this study has been included in the article, and no additional Supplementary Materials containing the data set are provided.

AUTHOR CONTRIBUTIONS

JC and JZ conceived the idea for this study, built the model, contributed to the simulation analysis, and wrote the manuscript. JC, ZJ, and KT contributed to manuscript preparation and figure preparation. YF, JZ, and YL contributed to data analysis, language, and thesis writing. All authors have read and agreed to the published version of the manuscript.

FUNDING

This work was supported by the NSFC (No.52075162), The Innovation Leading Program of New and High-tech Industry of Hunan Province (2020GK2015 and 2021GK4014), The Joint Fund Project of the Ministry of Education, The Excellent Youth Fund of Hunan Province (2021JJ20018), the Huxiang Youth Talent Project (2019RS2062), the Key Research & Development Program of Guangdong Province (2020B0101040002), the Natural Science Foundation of Changsha (kq2007026), the Engineering Physics and Science Research Council of the United Kingdom (EPSRC EP/P018998/1), and International Exchange Grant (IEC/NSFC/201078) through Royal Society and the NSFC.

REFERENCES

Adorno, S., Cerini, F., and Vercesi, F. (2022). "Microphones," in *Silicon Sensors and Actuators* (Cham: Springer), 503–522. doi:10.1007/978-3-030-80135-9_15

Anzinger, S., Bretthauer, C., Tumpold, D., and Dehe, A. (2021). A Non-linear Lumped Model for the Electro-Mechanical Coupling in Capacitive MEMS Microphones. *J. Microelectromechanical Syst.* 30 (3), 360–368. doi:10.1109/jmems.2021.3065129

Arora, N., Zhang, S. L., Shahmiri, F., Osorio, D., Wang, Y.-C., Gupta, M., et al. (2018). SATURN: A Thin and Flexible Self-Powered Microphone Leveraging Triboelectric Nanogenerator. *Proc. ACM Interact. Mob. Wearable Ubiquitous Technol.* 2 (2), 1–28. doi:10.1145/3214263

Auliya, R. Z., Buyong, M. R., Yeop Majlis, B., Mohd. Razip Wee, M. F., and Ooi, P. C. (2019). Characterization of Embedded Membrane in Corrugated Silicon Microphones for High-Frequency Resonance Applications. *Microelectron. Int.* 36 (4), 137–142. doi:10.1108/MI-02-2019-0010

Bi-Qiang, Y. U., Weng, H. S., Jiang, L. I., and Qiu, L. F. J. J. O. M. D. (2006). Coupling Design Modeling of MEMS Multi-Physics Region Based on MDO. *J. Mach. Design* 23 (11), 10–12.

Bogue, R., and Review, R. J. S. (2013). Recent Developments in MEMS Sensors: a Review of Applications, Markets and Technologies. *Mark. Technol.* 33 (4), 300–304. doi:10.1108/sr-05-2013-678

Choe, H. C., and Bulat, E. S. (2005). Systems and Methods for Sensing an Acoustic Signal Using Microelectromechanical Systems Technology. *J. Acoust. Soc. Am.* 118 (1), 25. doi:10.1121/1.1999410

Esteves, J., Rufer, L., Ekeom, D., and Basrour, S. (2017). Lumped-parameters Equivalent Circuit for Condenser Microphones Modeling. *J. Acoust. Soc. Am.* 142 (4), 2121–2132. doi:10.1121/1.5006905

Fitzgerald, A. M., White, C. D., and Chung, C. C. (2021). "Economics of Semiconductor Device Manufacturing and Impacts on MEMS Product Development," in *MEMS Product Development* (Cham: Springer), 9–16. doi:10.1007/978-3-030-61709-7_2

Kapps, C. A., and Dobbins, L. W. (2014). The 2010 Benjamin Franklin Medal in Electrical Engineering Is Presented to Gerhard M. Sessler and James E. West for the Invention and Development of the Electret Microphone. *J. Frankl. Inst.* 351 (1), 17–31. doi:10.1016/j.jfranklin.2012.12.006

Lee, J., Je, C. H., Yang, W. S., and Kim, J., (2012). "Structure-based Equivalent Circuit Modeling of a Capacitive-type MEMS Microphone," in 2012 International Symposium on Communications and Information Technologies (ISCIT) (IEEE), 2-5 Oct. 2022, Gold Coast, QLD, Australia, 228–233.

Lee, J., Im, J.-P., Kim, J.-H., Lim, S.-Y., and Moon, S.-E. (2019). Wafer-Level-Based Open-Circuit Sensitivity Model from Theoretical ALEM and Empirical OSCM Parameters for a Capacitive MEMS Acoustic Sensor. *Sensors* 19 (3), 488. doi:10.3390/s19030488

Mackey, A., Hicks, B., and Sullivan, D. M., (2019). *Microphone Cavity*. U.S. Patent, 10, 086.405

Mohd Ghazali, F. A., Hasan, M. N., Rehman, T., Nafea, M., Mohamed Ali, M. S., and Takahata, K. (2020). MEMS Actuators for Biomedical Applications: a Review. *J. Micromech. Microeng.* 30 (7), 073001–073020. doi:10.1088/1361-6439/ab8832

Naderyan, V., Raspet, R., and Hickey, C. (2021). Analytical, Computational, and Experimental Study of Thermoviscous Acoustic Damping in Perforated Micro-electro-mechanical Systems with Flexible Diaphragm. *J. Acoust. Soc. Am.* 150 (4), 2749–2756. doi:10.1121/10.0006378

Naderyan, V., Raspet, R., and Hickey, C. (2020). Thermo-viscous Acoustic Modeling of Perforated Micro-electro-mechanical Systems (MEMS). *J. Acoust. Soc. Am.* 148 (4), 2376–2385. doi:10.1121/10.0002357

Oh, S., Davaji, B., Richie, J., Lal, A., and Lee, C. H., (2021). "A Kirigami MEMS Velocity Acoustic Transducer," in 2021 21st International Conference on Solid-State Sensors, Actuators and Microsystems (Transducers) (IEEE), 20-24 June 2021, Orlando, FL, USA, 1319–1322.

Ozdogan, M., Towfighian, S., and Miles, R. N. (2020). Modeling and Characterization of a Pull-In Free MEMS Microphone. *IEEE Sensors J.* 20 (12), 6314–6323. doi:10.1109/jsen.2020.2976527

Resound, G. N. (2014) *Knowles Ships Two Millionth MEMS Microphone - Hearing Review*. knowles; Starkey, Eden Prairie, Minnesota, United States

Sant, L., Gaggl, R., Bach, E., Buffa, C., De Milleri, N., Sträussnigg, D., et al. (2019). "MEMS Microphones: Concept and Design for Mobile Applications," in *Low-Power Analog Techniques, Sensors for Mobile Devices, and Energy Efficient Amplifiers* (Springer), Berlin/Heidelberg, Germany, 155–174. doi:10.1007/978-3-319-97870-3_8

Shubham, S., Seo, Y., Naderyan, V., Song, X., Frank, A., Johnson, J., et al. (2021). A Novel MEMS Capacitive Microphone with Semiconstrained Diaphragm Supported with Center and Peripheral Backplate Protrusions. *Micromachines* 13 (1), 22. doi:10.3390/mi13010022

Wang, Y.-H., Chen, C.-P., Chang, C.-M., Lin, C.-P., Lin, C.-H., Fu, L.-M., et al. (2009). MEMS-Based Gas Flow Sensors. *Microfluid Nanofluid* 6 (3), 333–346. doi:10.1007/s10404-008-0383-4

Zhang, G., Ji, X., Li, X., Qu, G., and Xu, W. (2021). "EarArray: Defending against DolphinAttack via Acoustic Attenuation," in Network and Distributed Systems Security (NDSS) Symposium, February 21-25, 2021.

Conflict of Interest: The authors declare that the research was conducted in the absence of any commercial or financial relationships that could be construed as a potential conflict of interest.

Publisher's Note: All claims expressed in this article are solely those of the authors and do not necessarily represent those of their affiliated organizations, or those of the publisher, the editors, and the reviewers. Any product that may be evaluated in this article, or claim that may be made by its manufacturer, is not guaranteed or endorsed by the publisher.